The Golgi-associated COPI-coated buds and vesicles contain β/γ-actin

Ferran Valderrama*†, Ana Luna*†, Teresa Babià†, José A. Martínez-Menárguez‡, José Ballesta‡, Holger Barth§, Christine Chaponnier¶, Jaime Renau-Piqueras‖, and Gustavo Egea*,**

*Departament de Biologia Cellular, Facultat de Medicina, Institut d'Investigacions Biomediques August pi i Sunyer (IDIBAPS), Universitat de Barcelona, 08036 Barcelona, Spain; ‡Departamento de Biología Celular, Facultad de Medicina, Universidad de Murcia, 30071 Murcia, Spain; §Institut für Pharmakologie und Toxikologie, Albert-Ludwigs-Universität Freiburg, 79104 Freiburg, Germany; ¶Department of Pathology, University of Geneva, CH-1211 Geneva 4, Switzerland; and ‖Centro de Investigación, Hospital La Fe, 46009 Valencia, Spain

Edited by Kai Simons, European Molecular Biology Laboratory, Heidelberg, Germany, and approved December 6, 1999 (received for review August 10, 1999)

It has been shown previously that the morphology and subcellular positioning of the Golgi complex is controlled by actin microfilaments. To further characterize the association between actin microfilaments and the Golgi complex, we have used the *Clostridium botulinum* toxins C2 and C3, which specifically inhibit actin polymerization and cause depolymerization of F-actin in intact cells by the ADP ribosylation of G-actin monomers and the Rho small GTP-binding protein, respectively. Normal rat kidney cells treated with C2 showed that disruption of the actin and the collapse of the Golgi complex occurred concomitantly. However, when cells were treated with C3, the actin disassembly was observed without any change in the organization of the Golgi complex. The absence of the involvement of Rho was further confirmed by the treatment with lysophosphatidic acid or microinjection with the constitutively activated form of RhoA, both of which induced the stress fiber formation without affecting the Golgi complex. Immunogold electron microscopy in normal rat kidney cells revealed that β- and γ-actin isoforms were found in Golgi-associated COPI-coated buds and vesicles. Taken together, the results suggest that the Rho signaling pathway does not directly regulate Golgi-associated actin microfilaments, and that β- and γ-actins might be involved in the formation and/or transport of Golgi-derived vesicular or tubular intermediates.

Cytoplasmic and submembrane actin microfilaments are organized in linear bundles, two-dimensional nets, and three-dimensional gels. Actin isoforms segregate to functional regions of the cell in vertebrates and show slight functional differences *in vitro*. In particular, α isoforms are found in skeletal, cardiac, and vascular smooth muscles, γ isoform is found in enteric smooth muscle, and β and γ isoforms are present in the cytoplasm of non-muscle cells (ref. 1 and references therein). In addition, through actin cytoskeleton rearrangement, members of the Rho family Cdc42, Rac, and Rho proteins regulate the formation of filopodia, ruffles, and stress fibers, respectively (2).

Recently, actin and actin-associated proteins have been implicated in regulating the membrane dynamics of the Golgi complex (3–20). Actin-disrupting drugs have been used widely to show the involvement of actin in the endocytic pathway (ref. 20 and references therein). However, the role of actin in the secretory pathway is controversial. For example, treatment with cytochalasin D does not affect the Golgi-to-plasma membrane transport of either the VSVG protein, when monitored by fluorescence-activated cell sorter analysis (10), or the glycosaminoglycans release in the culture medium (20). However, cytochalasin B alters the *in vivo* formation of VSVG-GFP transport intermediates from Golgi membranes (21). Recently, using an *in vitro* assay, diverse isoforms of actin-binding proteins have been resolved biochemically in Golgi enriched fractions. It has also been shown that the newly budded and coated vesicles from Golgi membranes can bind to actin *in vitro* (18).

Clostridium botulinum toxins C2 and C3 depolymerize F-actin by ADP ribosylation of G-actin monomers and the small GTP-binding proteins Rho, respectively (22–24). We have found that the treatment with C2 toxin in normal rat kidney cells (NRK cells) led to a simultaneous disassembly of actin microfilaments and the collapse of the Golgi complex. The collapse of the Golgi complex is defined as the loss of the characteristic reticular and perinuclear morphology into a circular and more compact structure located in the centriolar region (ref. 10; see Fig. 1*G*). This criterion is used to define the reorganization of the Golgi complex on depolymerization of actin by C2. C3, on the other hand, caused actin disassembly without affecting Golgi complex. This suggests that, although actin is involved in the organization of the Golgi complex, this regulation is independent of Rho. Additionally, immunogold electron microscopy of intact cells revealed the presence of β- and γ-actin isoforms in Golgi-derived COPI-coated buds and vesicles. The significance of these findings is described below.

Materials and Methods

Materials. DMEM and FCS were from GIBCO/BRL Life Technologies (Paisley, Scotland); secondary tetramethylrhodamine B isothiocyanate (TRITC) or FITC $F(ab')_2$ fragments were from Boehringer Mannheim; phalloidin-TRITC, cytochalasin D, and lysophosphatidic acid were from Sigma. [^{32}P]NAD was purchased from Amersham Pharmacia. C3 exoenzyme was from Cytoskeleton (Denver). All other chemicals, if not otherwise stated were from Sigma and/or Merck.

Cell Culture. NRK cells were cultured in DMEM supplemented with 10% FCS. The cells were grown at 37°C in a humidified atmosphere of 5% CO_2.

Starvation Culture Conditions. Unlike Swiss 3T3 (25), NRK cells are resistant to clarifying of the cytoplasm of stress fibers in serum-deprived culture medium. Consequently, we thus developed the following protocol: Cells were prepared by seeding onto glass coverslips in tissue culture wells or Petri dishes containing DMEM/10% FCS. After the cell attachment, cells were washed three times in DMEM with $NaHCO_3$ without FCS (starvation medium) and were incubated for 48 h. Thereafter, the medium was removed, and cells were briefly incubated in the starvation medium containing cytochalasin D (5 μM, final concentration; 5 min, 37°C). To remove cytochalasin D, three washes were performed in starvation medium, and cells were

This paper was submitted directly (Track II) to the PNAS office.

Abbreviations: TRITC, tetramethylrhodamine B isothiocyanate; NRK cell, normal rat kidney cell; Man II, mannosidase II.

†F.V. and A.L. contributed equally to this study.

**To whom reprint requests should be addressed at: Departament de Biologia Cel.lular i Anatomia Patològica, Facultat de Medicina, Universitat de Barcelona, C/Casanova, 143, 08036 Barcelona, Spain. E-mail: egea@medicina.ub.es.

The publication costs of this article were defrayed in part by page charge payment. This article must therefore be hereby marked "*advertisement*" in accordance with 18 U.S.C. §1734 solely to indicate this fact.

further incubated in freshly prepared starvation medium for 1–3 days.

Incubation and Microinjection of C2 and C3 Toxins. Cell culture experiments: Botulinum toxin C2 (100 ng/ml of the catalytic subunit and 200 ng/ml of the binding component, final concentrations) or botulinum toxin C3 (20 μg/ml, final concentration) were added to NRK cells cultured in DMEM supplemented with 10% FCS at 37°C. Microinjection experiments: NRK cells were grown to 50–70% confluence on Eppendorf Cellocate Coverslips. The coverslips were transferred to a Petri dish containing culture medium buffered with 25 mM Hepes. C3 toxin was diluted in microinjection buffer (100 mM KCl/5 mM Hepes, pH 7.25) and was centrifuged at 14,000 $\times$ *g* at 4°C for 10 min. Cells were microinjected with an Automated Microinjection System (model 5242, Eppendorf). The coverslips were then transferred to a Petri dish containing fresh culture medium and were returned to the incubator for 10 min. Coverslips were then processed for immunofluorescence as described below.

Immunofluorescence. Toxin-treated and nontreated NRK cells were quickly washed in PBS (0.01M phosphate buffer/0.15 M NaCl, pH 7.2) and were fixed in freshly prepared paraformaldehyde (4% in PBS) at room temperature for 15 min. Cells were then washed 3 $\times$ 5 min, in PBS, and then in PBS containing ammonium chloride. The cells were then rinsed in PBS and were permeabilized with PBS containing 0.1% saponin and 0.1% BSA for 15 min. Cells were further processed for double-label immunofluorescence by using the rabbit polyclonal anti-mannosidase II (Man II) (1:4,000) and TRITC-phalloidin (diluted 1:250 from a stock solution of 0.2 mg/ml). Polyclonal antibodies were visualized with FITC anti-rabbit Ig F(ab′)2 fragments (1:30). The preparations were examined with an Olympus BX60 epifluorescence microscope and with a Leica TCS-NT confocal microscope. The quantitative assay for the Golgi complex morphology was performed as follows: normal Golgi complex morphology was defined as the subcellular structure (immunolabeled for Man II) with the characteristic perinuclear and reticular morphology with a minimum extension of the half of the nucleus profile. Collapsed Golgi complex was then defined as both a juxtanuclear compacted structure (Fig. 4*A*, arrows) and a relatively reticular structure but one in which immunolabel for Man II covered less than half of the nuclear profile. Two hundred cells per experimental condition were examined each time. Quantitative analysis was performed on randomly chosen microscopic fields on blind coded coverslips.

Immunoelectron Microscopy. NRK cells were processed for cryosectioning as described (26). In brief, the cells were fixed overnight with 4% paraformaldehyde in 0.1 M phosphate buffer, were pelleted by centrifugation, were embedded in 10% gelatin, and were cut into small blocks. The blocks were infused with 2.3 M sucrose, were frozen in liquid nitrogen, and were stored for cryoultramicrotomy. Cryosections were single or double immunolabeled with rabbit polyclonal antibodies followed by protein A-gold (26). β-actin was detected by using the antibody β74, and γ-actin was detected by the antibody AAL20 (27); the β component of the coatomer (β-COP) was revealed with a polyclonal antibody, a gift from T. Kreis (University of Geneva). To establish the relative distribution of β-actin in the Golgi (Table 1), gold particles were counted and ascribed to one of the following categories: Golgi stack, Golgi vesicles, or nonmembrane associated. Randomly selected Golgi areas (a total of 30) were studied. The number of gold particles found for each category was expressed as a percentage. To study the type of Golgi vesicles associated with β-actin (Table 2), we counted 75 vesicles positive for β-actin. The type of coat was established in the basis of thickness and appearance (28, 29). The relative distribution of β-actin within the Golgi stack was also studied (Table 3). Gold particles were counted and ascribed to one of the following categories: COP-coated buds, lateral rims (lateral portions of the cisterna showing the characteristic dilatation), or flattened central portion of the cisternae. Samples were visualized in a Zeiss EM10 electron microscope. Statistical analysis was performed with the Student's *t* test.

Fluorescent Phalloidin Binding Assay. Control and poisoned NRK cell cultures were fixed in 4% paraformaldehyde in PBS for 15–30 min and permeabilized with 0.1% Triton X-100 in PBS for 5 min. After 3 rinses in PBS, cells were incubated with TRITC-phalloidin (1:1,000 from a stock solution of 0.2 mg/ml) in PBS for 15 min, washed 3 times in PBS, and extracted with methanol for 25 min at room temperature. The fluorescence intensity of the supernatants was measured in a Kontron Instruments fluorimeter (SFM25) at 554 nm and 573 nm (excitation and emission).

[^{32}P]ADP-Ribosylation Assay. NRK cells were incubated with C3 exoenzyme (20 μg/ml) for various times. Cells were washed twice by centrifugation (1,000 $\times$ *g* for 5 min) in complete medium and were lysed by periodic agitation for 15 min in ice-cold lysis buffer (50 mM Tris·HCl/120 mM NaCl/2.5 mM EDTA/1 mM DTT/0.5% Nonidet P-40, pH 7.4) containing protease inhibitors (200 mM phenylmethylsulfonyl fluoride and 5 μg/ml leupeptin) and phosphatase inhibitors (1 mM sodium fluoride, 1 mM sodium orthovanadate, and 10 mM β-glycerophosphate). After centrifugation (16,000 $\times$ *g* for 10 min) the supernatant (corresponding to 80 μg of protein) was incubated (30) with 53 μl of ribosylation buffer (150 mM Tris·HCl/30 mM nicotinamide/15 mM thymidine/15 mM DTT/7.5 mM $MgCl_2$/10 μM [^{32}P]NAD, pH 8.0) in the absence or presence of 7.5 ng of recombinant C3 exoenzyme. The samples were mixed with 14 μl of 5$\times$ sample buffer (125 mM Tris/4% SDS/20% glycerol/10% 2-mercaptoethanol/0.01% bromophenacyl blue, pH 6.8), were boiled for 5 min, and were subjected to SDS/PAGE using a 5% stacking gel and a 15% separating gel. The proteins were electrophoretically transferred to nitrocellulose membranes and subjected to autoradiography.

Results and Discussion

C2 Treatment Induces Disassembly of Actin Microfilaments and the Collapse of the Golgi Complex. C2 is an ADP ribosyltransferase that modifies monomeric G-actin but not polymerized F-actin (35). It enters the cells by receptor-mediated endocytosis (30). A time course of treatment with C2 toxin added in the culture medium showed a correlation between the depolymerization of actin and the collapse of the Golgi complex (Fig. 1). For example, after 2 h of treatment, the onset of the Golgi collapse (Fig. 1*C*) was observed simultaneously with a slight loss of actin filament integrity (Fig. 1*D*). After 4 h, the morphological alterations were more pronounced. In particular, the Golgi complex was more compact (Fig. 1*E*), and there was an extensive disassembly of actin stress fibers (Fig. 1*F*). After 6 h, the actin filaments were severely disassembled (Fig. 1*H*), and Golgi complex was found as a tightly collapse morphology (Fig. 1*G*). Notably, the Golgi complex collapse was produced without significant changes in the cellular shape (Fig. 1 *F* and *H*). A quantitative analysis of the alterations in the Golgi complex and F-actin content after C2 treatment was performed (Fig. 2*A*). The percentage of the Golgi complex with its characteristic reticular and perinuclear morphology (Fig. 1*A*) diminished in parallel to the F-actin content (Fig. 2*A*). When C2 toxin was microinjected into the cytoplasm, we observed a concomitant collapse of the Golgi complex (Fig. 4*A*, small arrows) and the disruption of actin (Fig. 4*B*, small

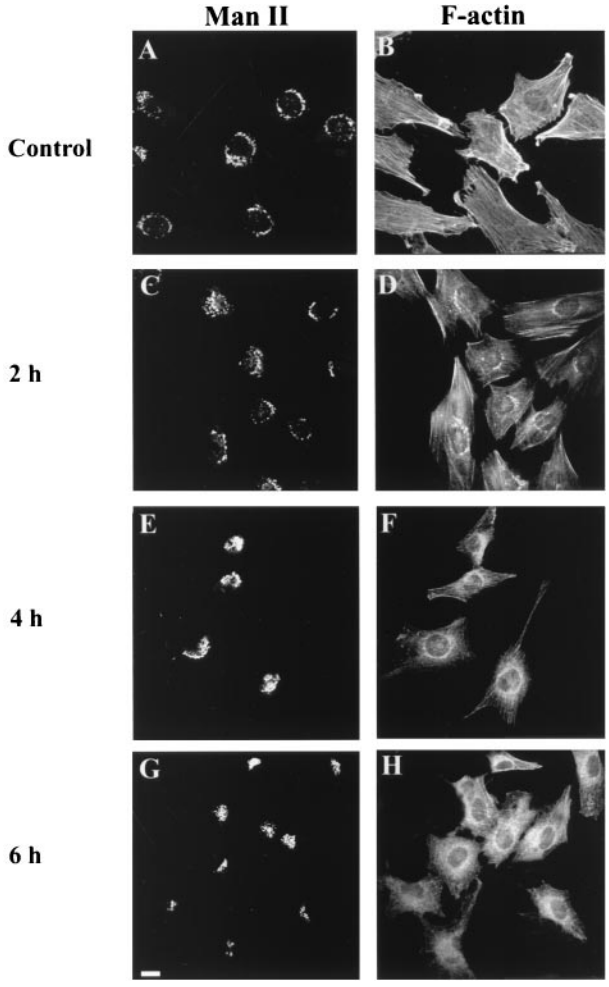

Fig. 1. Confocal fluorescence microscopy of control (*A* and *B*) and C2-poisoned (*C–H*) NRK cells stained with antibodies to Man II (*A*, *C*, *E*, and *G*) and with TRITC-phalloidin (*B*, *D*, *F*, and *H*). Note the concomitant collapse of the Golgi complex and the stress fiber disruption when the toxin was being added into the culture medium.

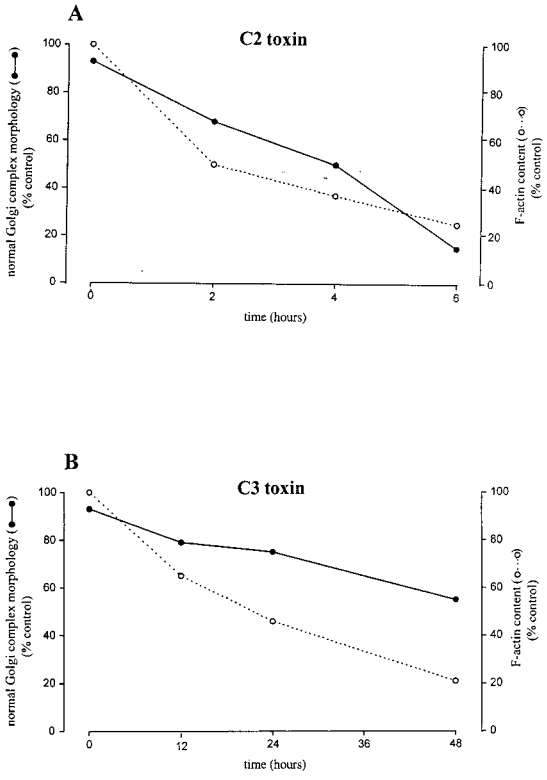

Fig. 2. Quantitative analysis of the percentage of normal Golgi complex morphology (see Figs. 1*A* and 5*A*) and F-actin content measured by the phalloidin binding assay at different incubation times with C2 (*A*) or C3 (*B*) toxins. Results are the mean of duplicate experiments.

arrows). Together, these results show an interaction between actin microfilaments and the Golgi complex. This is consistent with our previous observations (10, 11, 20).

***In Situ* Immunolocalization of β- and γ-Actin Isoforms to Golgi-Associated COP-Coated Buds and Vesicles.** C2 transferase alters the non-muscle β/γ and not the α-G-actin isoform (31, 32). Thus, only actin microfilaments containing β/γ isoforms should be perturbed by C2, and, therefore, C2 treatment should affect the subcellular structures linked only to these isoforms. Our findings with C2 toxin suggest that the Golgi complex is associated with the β/γ actin microfilaments. Staining with β- and γ-actin antibodies at the fluorescence microscopy level did not show a clear Golgi staining. This is because these actin isoforms are abundant cytoplasmic proteins and may mask the small but specific interaction to Golgi membranes. We, therefore, examined the subcellular localization of β- and γ-actin isoforms in NRK cells by cryoimmunoelectron microscopy. We describe and illustrate the immunolabeling for β-actin only, although similar results were also obtained with the γ-actin antibodies (data not shown). Anti-β actin antibodies strongly labeled cortical actin bundles (Fig. 3*A*, arrows) and non-membrane-associated structures (Fig. 3 *A* and *D*; Table 1), the latter probably reflecting the cytoplasmic network of actin microfilaments. More importantly, gold labeling was visualized in the Golgi cisternae and associated structures (Fig. 3 *B–E*; Table 3;). Gold particles were also visualized in both COP-coated vesicles and budding profiles emerging from rims of the cisternae (Fig. 3 *C* and *E*, arrows; Table 2). COP-coated structures were initially identified by the shape and size of the coat that is clearly distinguishable from the clathrin coat (refs. 28 and 29; Fig. 3*D*, arrowhead; Table 2). Double immunogold labeling experiments confirmed that β-actin colocalized in COPI-coated membranes (Fig. 3 *D* and *E*, arrows). The quantitative analysis of the gold labeling in the Golgi stack demonstrated a preferential association of β/γ actins in the lateral rims and buds of Golgi cisterna, representing both together the 80% of the total gold labeling for β-actin (Table 3). In a recent report (18), it has been shown by immunoblotting techniques that fractions of Golgi membranes and vesicles contain β-actin. Although this is a good indication of the presence of actin in Golgi membranes and derived structures, the possibility of another membrane compartments in the Golgi-enriched fractions cannot be ruled out. We state this because (*i*) Golgi enriched fractions also contain endosomes and plasma membrane, and (*ii*) COPI coats are also found in endosomes (33, 34). Interestingly, there was a significant labeling of noncoated vesicles and/or tubules (Table 2; Fig. 3 *C* and *D*). Because the COPI coat is quickly lost after vesicle formation, these uncoated structures most probably represent naked COPI-coated membrane transport intermediates. Therefore, the results with C2 toxin and immunolocalization of β/γ actin to Golgi complex and Golgi-derived structures in intact cells are conclusive of the association of actin microfilaments with the Golgi complex.

C3 Induces the Disassembly of Actin Stress Fibers but Does Not Alter the Reticular and Perinuclear Morphology of the Golgi Complex. The small GTP-binding protein Rho controls the stress fiber forma-

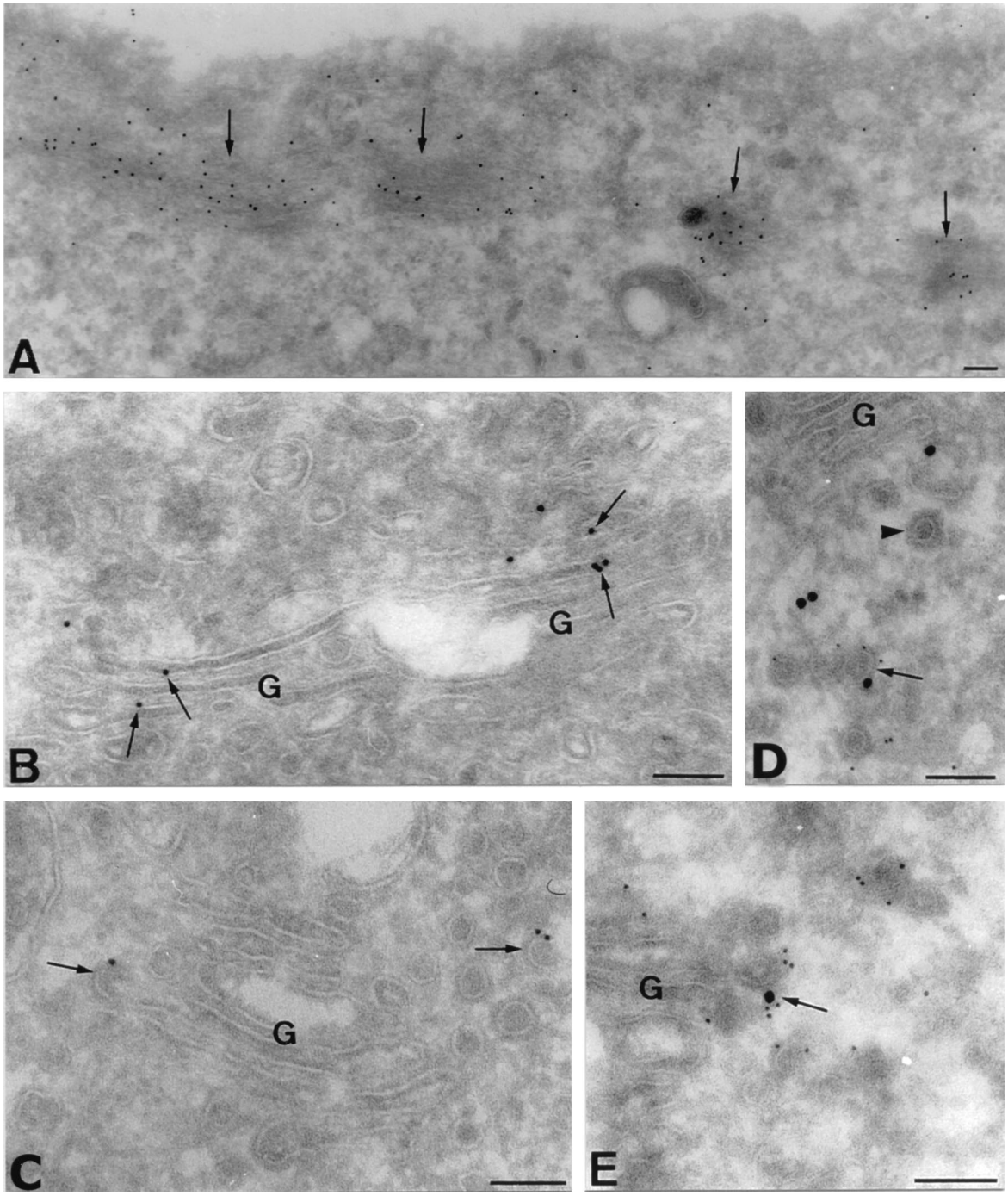

Fig. 3. Ultrathin cryosections of NRK cells single immunolabeled for β-actin isoform (10 nm gold) (*A–C*), and double immunolabeled for β-actin (15 nm gold) and β-COP (5 nm gold) (*D* and *E*). Bundles of actin microfilaments running under the plasma membrane are strongly labeled for β-actin (*A*, arrows). (*B* and *C*) β-actin is also associated with Golgi membranes. Gold particles are preferentially visualized in the lateral rims of the cisternae (*B*, arrows), in COP-coated buds (*C*, left arrow), and in COP-coated vesicles (*C*, right arrow). (*D* and *E*) COPI-coated buds and vesicles contain β-actin. β-Actin and β-COP colocalize in Golgi-associated vesicles (*D*, arrow). Arrowhead in *D* shows a nonlabeled clathrin-coated vesicle. (*E*) Detail of a COPI-coated bud labeled for β-actin emerging from the rim of a Golgi cisternae (arrow). G, Golgi stack. (Bars = 100 nm.)

Table 1. Subcellular distribution of β-actin in the Golgi complex: Golgi area

Golgi stack	Vesicles	Non-membrane bound
29.3 ± 5.6	44.5 ± 6.6*	26.2 ± 5.7*

Numbers represent the percentages (mean ± SEM) of the total labeling in distinct locations in the Golgi area. *, $P \leq 0.03$.

tion (35). C3 exoenzyme inactivates Rho by ADP ribosylation (36). To examine whether Rho regulates the Golgi-associated actin microfilaments, we incubated NRK cells with C3 and, as described previously for C2, monitored changes in the morphology of the Golgi complex and F-actin integrity (Fig. 5). In C3-treated cells, the Golgi complex retained its characteristic reticular and perinuclear morphology (Fig. 5 *C*, *E*, and *G*). In contrast, the stress fibers were progressively disassembled (Fig.

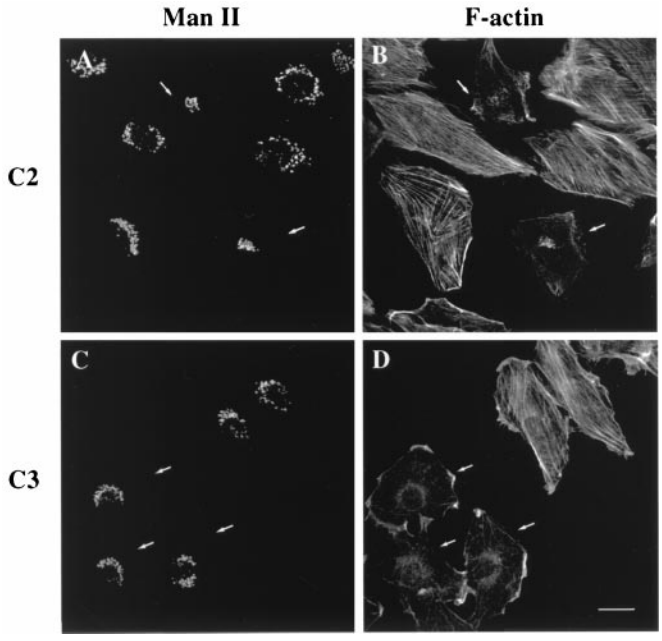

Fig. 4. Microinjection experiments with C2 (*A* and *B*) and C3 (*C* and *D*). The injection of C2 and C3 cause the rapid disassembly of actin stress fibers stained with TRITC-phalloidin (*B* and *D*). The Man II-stained Golgi complex (*A* and *C*) collapses in the presence of C2 (*A*) but not of C3 (*C*). Small white arrows indicate the microinjected cells. (Bar = 10 μm.)

5 *D*, *F*, and *H*). However, the time required for the C3 toxin to exert its effect was much longer than that for C2. C3 enters the cell by an unknown mechanism, and this lag in the toxic action may be attributable to delayed binding and the subsequent internalization. This is not the case when C3 is directly microinjected into the cytoplasm, where the toxic effect is produced in minutes (25). Consequently, we microinjected C3 toxin, and results obtained were identical (Fig. 4 *C* and *D*) to those observed when the toxin was added to culture medium (Fig. 5). A quantitative analysis showed that the decrease in F-actin content by C3-treatment (Fig. 2*B*) was not accompanied by a decrease in the percentage of the Golgi complex with normal morphology (Fig. 5*A*).

The biological effects of C3 exoenzyme correlate well with the extent of ADP ribosylation of Rho *in vivo* (37, 38). Consequently, the ability of C3 exoenzyme to ADP ribosylate Rho *in vivo* was also tested (Fig. 6) in parallel to immunocytochemical experi-

Table 2. Subcellular distribution of β-actin in the Golgi complex: Golgi vesicles

Clathrin-coated vesicles	COP-coated vesicles	Non-coated vesicles
5.2 ± 1.4*	31.1 ± 1.9*†	63.6 ± 1.1†

Numbers represent the percentages (mean ± SEM) of each type of vesicles labeled for β-actin. The type of vesicle was defined by using morphological criteria on the basis of thickness and appearance of the coat (18 nm and 10 nm for clathrin and COP, respectively). *, $P \leq 0.0004$. †, $P \leq 0.0001$.

Table 3. Subcellular distribution of β-actin in the Golgi complex: Golgi stack

Coated-buds	Lateral rims	Central portion
36.0 ± 6.1	44.0 ± 2.3*	20.0 ± 4.0*

Numbers represent the percentages (mean ± SEM) of gold particles in each subcompartment (see *Material and Methods*). *, $P \leq 0.006$.

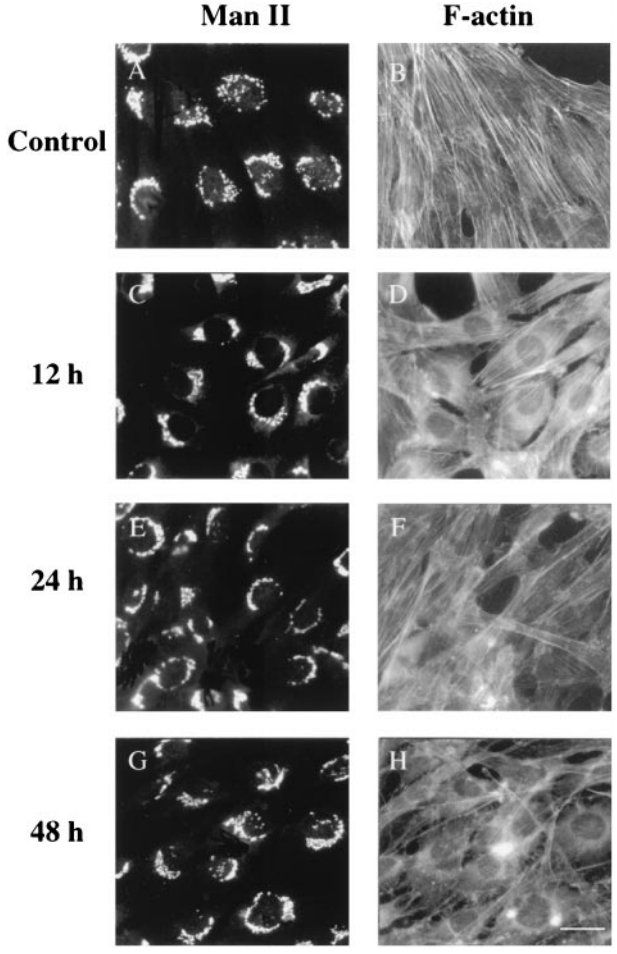

Fig. 5. Confocal fluorescence microscopy of control (*A* and *B*) and C3-treated (*C–F*) NRK cells stained with antibodies to Man II (*A*, *C*, *E*, and *G*) and with TRITC-phalloidin (*B*, *D*, *F*, and *H*). The C3-induced disassembly of the actin stress fibers does not alter the reticular and perinuclear morphology of the Golgi complex.

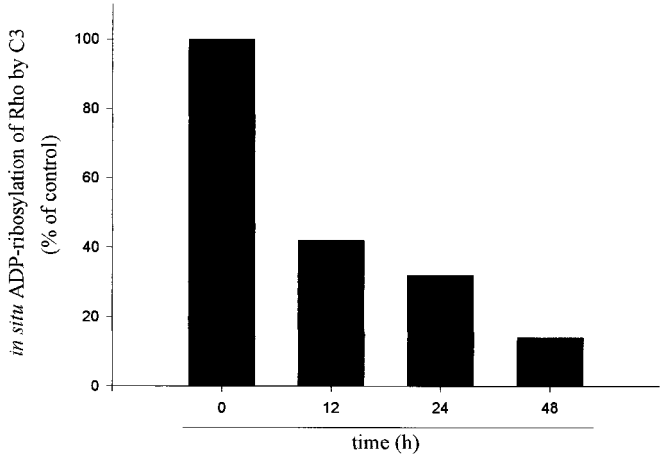

Fig. 6. ADP ribosylation of Rho by C3 toxin in NRK cells. NRK cells were incubated with C3 toxin at 20 μg/ml for 12, 24, and 48 h and were lysed. The lysates were subjected to a second treatment with C3 in the presence of [^{32}P]NAD and were separated by SDS/PAGE. The amount of [^{32}P]ADP ribosylated Rho was evaluated from the gel by a PhosphorImager (Molecular Dynamics) and was calculated as percentage of control. The decrease in [^{32}P]NAD incorporation reflects the degree of prior *in vivo* ADP ribosylation achieved with C3.

ments (Fig. 5). The amount of Rho ADP ribosylated *in vivo* was determined by *in vitro* ADP ribosylation of lysates of treated cells with [^{32}P]NAD. Once Rho is ADP ribosylated *in vivo*, it can no longer serve as a substrate for the *in vitro* ADP ribosylation reaction (39). The exposure of NRK cells to C3 exoenzyme caused a progressive ADP ribosylation of Rho *in vivo* (Fig. 6). After 48 h of incubation with C3, when the disassembly of actin was morphologically complete (Fig. 5*H*) and the F-actin content was at its lowest level (Fig. 3*B*), 86% of Rho was ADP ribosylated *in vivo*. It is important to note that >80% of ADP ribosylation of Rho is required to observe its biological effect (39). Taken together, the results suggest that Rho does not directly regulate the Golgi-associated actin cytoskeleton. In addition, microinjection of the constitutively actived form of RhoA (L63RhoA) or treatment with lysophosphatidic acid in starved NRK cells induced the stress fiber formation (35). We have found that these treatments did not affect the reticular morphology of the Golgi complex (data not shown). Taken together, results with C3 toxin, lysophosphatidic acid, and the constitutive form of RhoA indicate that Rho does not directly regulate the actin microfilaments that are associated with the Golgi complex and that they do not form part of stress fibers.

In conclusion, we show that (*i*) β- and γ-actin are found attached to COPI-coated buds and vesicles; (*ii*) C2 treatment affects both actin and Golgi organization; and (*iii*) C3 treatment affects actin but not Golgi complex. Taken together, these results show the direct involvement of specific isoforms of actin in regulating the organization of the Golgi complex and in the transport of membrane components by COPI-coated structure(s) in the anterograde/retrograde membrane pathway(s) and/or in the formation process of transport intermediates.

We thank Maite Muñoz for technical support, Robin Rycroft for editorial assistance, and Anna Bosch (Serveis Científico-Tècnics-Campus Casanova) for help with the confocal microscope. We also thank to Drs. G. Gabbiani for anti-β and anti-γ antibodies, the late T. Kreis for anti-β-COP antibodies, and A. Hall for the constitutive form of RhoA (L63RhoA). F.V. and A.L. are predoctoral fellows of the Universitat de Barcelona and IDIBAPS, respectively. J.A.M.-M. is supported by a postdoctoral fellowship from the Universidad de Murcia. These studies were supported by a Comisión Interministerial de Ciencia y Tecnología grant to G.E. (SAF 97-0016).

1. Sheterline, P., Clayton, J. & Sparrow, J. (1998) *Actin* (Oxford Univ. Press, Oxford), pp. 1–272.
2. Tapon, N. & Hall, A. (1997) *Curr. Opin. Cell Biol.* **9,** 86–92.
3. Beck, K., Buchanan, J., Malhotra, V. & Nelson, J. W. (1994) *J. Cell Biol.* **127,** 707–723.
4. Beck, K., Buchanan, J. & Nelson, JW. (1997) *J. Cell Sci.* **110,** 1239–1249.
5. Devarajan, P., Stabach, P., Mann, A., Ardito, T., Kashgarian, M. & Morrow, J. (1996) *J. Cell Biol.* **133,** 819–830.
6. Devarajan, P., Stabach, P., De Matteis, M. & Morrow, J. (1997) *Proc. Natl. Acad. Sci. USA* **94,** 10711–10716.
7. Fath, K., Trimbur, G. & Burgess, D. (1997) *J. Cell Biol.* **139,** 1169–1181.
8. Holleran, E. & Holzbaur, E. (1998) *Trends Cell Biol.* **8,** 26–29.
9. Stankewich, M., William, T., Peters, L., Ch'ng, Y., John, K., Stabach, P., Devarajan, P., Morrow, J. & Lux, S. (1998) *Proc. Natl. Acad. Sci. USA* **95,** 14158–14163.
10. Valderrama, F., Babià, T., Ayala, I., Kok, J., Renau-Piqueras, J. & Egea, G. (1998) *Eur. J. Cell Biol.* **76,** 9–17.
11. Babià, T., Ayala, I., Valderrama, F., Mato, E., Bosch, M., Santarén, J., Renau-Piqueras, J., Kok, J., Thomson, T. & Egea, G. (1999) *J. Cell Sci.* **112,** 477–489.
12. Baumann, O. (1998) *Cell Tissue Res.* **291,** 351–361.
13. Fath, K. & Burgess, D. (1993) *J. Cell Biol.* **120,** 117–127.
14. Ikonen, E., de Almeid, J., Fath, K., Burgess, D., Ashman, K., Simons, K. & Stow, J. L. (1997) *J. Cell Sci.* **110,** 2155–2164.
15. Montes de Oca, G., Lezama, R., Mondragón, R., Castillo, A. & Meza, I. (1997) *Arch. Med. Res.* **28,** 321–328.
16. Müsch, A., Cohen, D. & Rodríguez-Boulan, E. (1997) *J. Cell Biol.* **138,** 291–306.
17. Buss, F., Kendrick-Jones, J., Lionne, C., Knight, A., Cote, G. & Paul Luzio, J. (1998) *J. Cell Biol.* **143,** 1535–1545.
18. Heimann, K., Percival, J., Weinberger, R., Gunning, P. & Stow, J. L. (1999) *J. Biol. Chem.* **274,** 10743–10750.
19. Weiner, O., Murphy, J., Griffiths, G., Schleicher, M. & Noegel, A. (1993) *J. Cell Biol.* **123,** 23–34.
20. di Campli, A., Valderrama, F., Babià, T., De Matteis, M. A., Luini, A. & Egea, G. (1999) *Cell Motil. Cytoskeleton* **43,** 334–348.
21. Hirschberg, K., Miller, C. M., Ellenberg, J., Presley, J. F., Siggia, E. D., Phair, R. D. & Lippincott-Schwartz, J. (1999) *J. Cell Biol.* **143,** 1485–1503.
22. Aktories, K., Barmann, M., Ohishi, I., Tsuyama, S. & Jakobs, K. (1986) *Nature (London)* **322,** 390–392.
23. Aktories, K., Braun, U., Rosener, S., Just, I. & Hall, A. (1989) *Biochem. Biophys. Res. Commun.* **158,** 209–213.
24. Chardin, P., Boquet, P., Madaule, P., Popoff, M., Rubin, E. & Gill, D. (1989) *EMBO J.* **8,** 1087–1092.
25. Nobes & Hall, A. (1997) in *Bacterial Toxins (Tools in Cell Biology and Pharmacology)*, ed. Aktories, K. (Chapman & Hall, Weinheim), pp. 71–81.
26. Martínez-Menárguez, J. A., Geuze, H., Slot, J. & Klumperman, J. (1999) *Cell* **98,** 81–90.
27. Yao, X., Chaponnier, C., Gabbiani, G. & Forte, J. (1995) *Mol. Biol. Cell* **6,** 541–557.
28. Oprins, A., Duden, R., Kreis, T., Geuze, H. & Slot, J. (1993) *J. Cell Biol.* **121,** 49–59.
29. Martínez-Menárguez, J. A., Geuze, H. & Ballesta, J. (1996) *Eur. J. Cell Biol.* **71,** 137–143.
30. Simpson, L. (1989) *J. Pharmacol. Exp. Ther.* **251,** 1223–1228.
31. Mauss, S., Chaponnier, C., Just, I., Aktories, K. & Gabbiani, G. (1990) *Eur. J. Biochem.* **194,** 237–241.
32. Vandekerckhove, J., Schering, B., Barmann, M. & Aktories, K. (1988) *J. Biol. Chem.* **263,** 696–700.
33. Whitney, J. A., Gómez, M, Sheff, D., Kreis, T. E. & Mellman, I. (1995) *Cell* **83,** 703–713.
34. Aniento, F., Gu, F., Parton, R. G. & Gruenberg, J. (1996) *J. Cell Biol.* **133,** 29–41.
35. Ridley, A. & Hall, A. (1992) *Cell* **70,** 389–399.
36. Lemichez, E., Bouquet, P. & Popoff, M. (1997) in *Guidebook to Protein Toxins and Their Use in Cell Biology*, eds. Rappuoli, R. & Montecucco, C. (Springer, Heidelberg), pp. 36–37.
37. Yamamoto, M., Marui, N., Sakai, T., Morii, N., Kozaki, S., Ikai, K., Imamura, S. & Narumiya, S. (1993) *Oncogene* **8,** 1449–1455.
38. Tominaga, T., Sugie, K., Hirata, M., Morii, N., Fukata, J., Uchida, A., Imura, H. & Narumiya, S. (1993) *J. Cell Biol.* **120,** 1529–1537.
39. Saito, Y. & Narumiya, S. (1997) in *Bacterial Toxins (Tools in Cell Biology and Pharmacology)*, ed. Aktories, K. (Chapman & Hall, Weinheim), pp. 85–92.